Modeling morphological changes in spinal motoneurons after spinal cord injury to explore changes in electrical behavior

Joe Graham[1,2] & Ranu Jung[1,2]

[1]Center for Adaptive Neural Systems, [2]The Harrington Department of Bioengineering, Arizona State University, Tempe, AZ, USA,

ASU Arizona State University
IRA A. FULTON School of Engineering
designing adaptive engineered systems ... to promote adaptation in neural systems
CENTER FOR ADAPTIVE NEURAL SYSTEMS

Introduction and Specific Aims

Motoneurons and Morphology

Motoneurons are the final common pathway of motor control

All motor-related activity in the nervous system must ultimately converge on motoneurons

Motoneuron dendritic morphology is known to play an important role in determining motoneuron behavior [1]

Motoneuron dendritic morphology can be described parsimoniously by a set of recursive rules that inter-correlate local parameters [2]

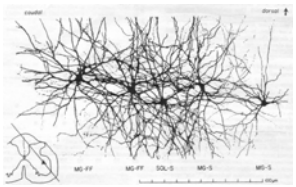

Figure 1. Normal medial gastrocnemius and soleus motoneurons from the cat. Note the extensive dendritic arborization. From [3].

Spinal Cord Injury and Motoneurons

Following a chronic spinal cord injury (SCI), motoneuron morphology changes [4,5]. On average:

- Soma size becomes larger
- Number of primary dendrites decreases
- Primary dendrite diameter increases
- Extent of dendritic arborization decreases

Motoneuron excitability is markedly increased following a chronic SCI [6,7]:

- Extended rhythmic firing during injected currents
- Long-lasting responses to reflex activation

To date, it is not clear how altered motoneuron morphology following SCI affects electrical behavior

Figure 2. Normal and chronic spinal cord transection (SCT) motoneurons from rat. Note the loss of dendritic arborization following SCT. From [2].

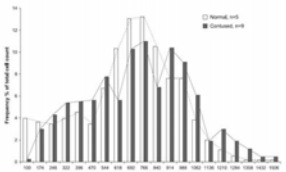

Figure 3. Normal and chronic SCI motoneurons soma size distributions for soleus in rat. Note the skew towards larger soma size following SCI. From [3].

Specific Aims

1. Quantify normal and SCI motoneuron morphology

2. Generate realistic digital morphologies for normal and SCI motoneurons

3. Use computational modeling techniques to explore the effects of altered morphology on electrical behavior

Long term goal: creation of morphologically realistic compartmental models of rat hindlimb motoneurons arranged into pools, for the normal and chronic SCI condition, which interface with a musculoskeletal model of the rat hindlimb

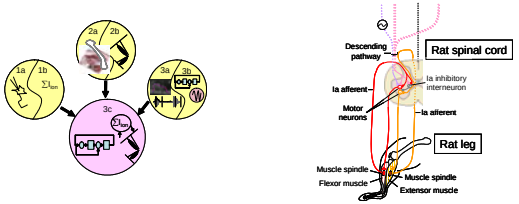

Figure 4. Long-term goals. Left: 1a/b: motoneuron electrophysiology, morphology, and modeling. 2a/b:Musculoskeletal morphology and modeling. 3a/b/c: connection of neural and musculoskeletal models. Right: components to be quantified and modeled.

Methods

Experimental Methods

Animals: Female adult (250-300g) Long Evans rats (Control n=10; T8 contusion (150-160Kdyne impact) n=20

Labeling: Spinal motoneurons retrogradely labeled via injection of fluorescein-conjugated cholera toxin β subunit (CTβ) 0.1% aqueous solution into the selected muscles: Alexafluor 594 "red" for **iliacus (IL)** and **tibialis anterior (TA)**, Alexafluor 488 "green" for **biceps femoris (BF)** and **gastrocnemius medialis (GM).**

Spinal Cord Harvesting: 72 hours post CTβ injection under deep anesthesia (40 mg/kg sodium pentobarbitol); perfused with 0.1 M phosphate-buffered saline, followed by 4% paraformaldehyde (PFA). Spinal cords removed, post-fixed in PFA for 24 hours, transferred to a 30% sucrose solution for 24 to 48 hours. Cords embedded and frozen for sectioning.

Histology: 40 µm cryosections examined using a fluorescent and a confocal microscope. Reconstructions using Neurolucida™ software.

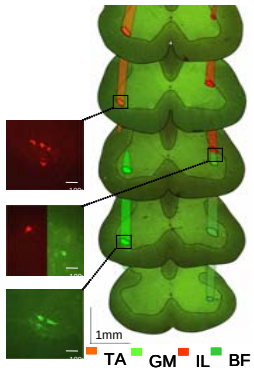

Figure 5. Labeled motoneurons and their positioning within the spinal cord as determined experimentally in uninjured rat.

Computational Methods

Motoneuron morphologies generated using L-Neuron

- Basic or "fundamental" parameters are sufficient to generate realistic neuronal morphologies
- These distributions are sampled iteratively to "grow" motoneuron morphologies from the soma outward
- All initial parameter distributions are from the literature
- Many final parameter distributions will be quantified experimentally

Morphologies quantified using output from L-Measure

- Emergent parameters are measured
- Distance and segment analyses performed

Iterative process of generation/quantification to refine morphologies

Digital morphologies imported into GENESIS or NEURON for computational modeling

Basic Parameters	Emergent Parameters
Soma diameter	Rostral-caudal extent
Number of primary dendrites	Dorsal-ventral extent
Diameter of primary dendrites	Medial-lateral extent
Dendritic taper rate	Dendritic length
Contraction and Fragmentation	Dendritic surface area
Length between bifurcations	Dendritic volume
Bifurcation threshold	Number of segments
Bifurcation angles	Number of terminations
Rall Power	Number of branch points
Poliko Constant	Maximum branch order
Daughter diameter ratio	Distance Analysis
Terminal branch pathlength	Segment Analysis

Table 1. Left: Basic parameter distributions needed to generate digital motoneuron morphologies using L-Neuron and the Hillman algorithm. Right: Emergent parameters quantified in L-Measure for comparison with actual motoneuron reconstructions.

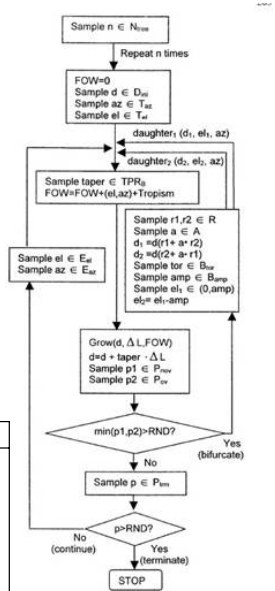

Figure 6. Recursive algorithm of Burke as implemented in L-Neuron in order to "grow" digital motoneuron morphologies from the soma outward. Basic parameter distributions are sampled at each step of the algorithm for each step of growth. From [2].

Preliminary Results

Experimental Results

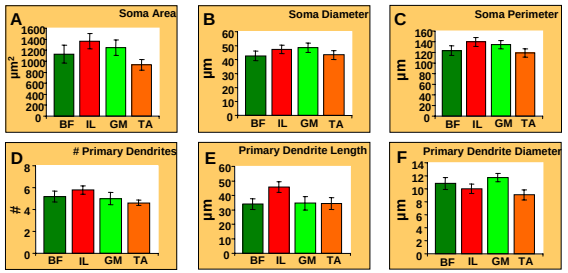

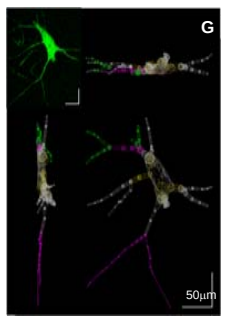

Figure 7. Experimentally quantified motoneuron morphological parameters from uninjured rat. Bars are standard error, data for A – F: n=1 animal, p=5 motoneurons, 2D measurements.
A: Soma area (µm²)
B: Soma diameter: maximum diameter of the soma (µm)
C: Number of primary dendrites
D: Soma perimeter (µm)
E: Primary dendrite length: mean length of the primary dendrites measured from soma to first branch point.
F: Primary dendrite diameter: mean value of the maximum diameter of primary dendrites (µm)
G: 3D motoneuron reconstruction. Top left: flattened confocal stack acquired with minimum 1.0 µm resolution. Other views are orthogonal representations of 3D reconstruction performed with Neurolucida software. All scale bars are 50 µm.

Computational Results

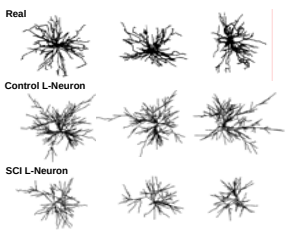

Figure 8. Orthogonal views of representative motoneuron morphologies. Top row is actual reconstructions from rat from [8]. Middle row is L-Neuron generated morphologies for the control case. Bottom row is L-Neuron generated morphologies for the SCI case, with mean soma diameter increased by 18%, number of primary dendrites reduced by 22%, and primary dendrite diameter increased by 20%, as seen experimentally in Bose and Gazula and Kitzman.

Parameter	Control	SCI
Soma Surface Area (μ m^2)	7685	10768
Number of Primary Dendrites	12.0	8.8
Number of Bifurcations	153.2	133.0
Number of Branches	329.4	282.6
Number of Terminations	165.2	141.8
Maximum Branch Order	12.6	10.2

Table 2. Emergent parameters for control and SCI conditions with 5 generated motoneuron morphologies in each group. Note that several measures of dendritic arborization emergent parameters are decreased in the SCI case.

References

1.van Ooyen, A., et al., The effect of dendritic topology on firing patterns in model neurons. Network, 2002. 13(3): p. 311-25.

2. Ascoli, G.A. and J.L. Krichmar, L-neuron: A modeling tool for the efficient generation and parsimonious description of dendritic morphology. Neurocomputing, 2000. 32-33: p. 1003-1011.

3. Henneman, E. and L.M. Mendell, Functional Organization of the Motoneuron Pool and its Inputs. Handbook of Physiology.

4. Bose, P., et al., Morphological changes of the soleus motoneuron pool in chronic midthoracic contused rats. Exp Neurol, 2005. 191(1): p. 13-23.

5. Gazula, V.R., et al., Effects of limb exercise after spinal cord injury on motor neuron dendrite structure. J Comp Neurol, 2004. 476(2): p. 130-45.

6. Beaumont, E., et al., Passive exercise and fetal spinal cord transplant both help to restore motoneuronal properties after spinal cord transection in rats. Muscle Nerve, 2004. 29(2): p. 234-42.

7. Bennett, D.J., Y. Li, and M. Siu, Plateau potentials in sacrocaudal motoneurons of chronic spinal rats, recorded in vitro. J Neurophysiol, 2001. 86(4): p. 1955-71.

8. Chen, X.Y. and J.R. Wolpaw, Triceps surae motoneuron morphology in the rat: a quantitative light microscopic study. J Comp Neurol, 1994. 343(1): p. 143-57.

Supported in part by NIH NS054282-01